ARTICLE
Journal of Cellular Biochemistry 114:2007–2015 (2013)

Journal of Cellular Biochemistry

RING Finger Protein 10 Regulates Retinoic Acid-Induced Neuronal Differentiation and the Cell Cycle Exit of P19 Embryonic Carcinoma Cells

Yousra S. Malik, Muhammad A. Sheikh, Mingming Lai, Rangjuan Cao, and Xiaojuan Zhu*

Key Laboratory of Molecular Epigenetics of Ministry of Education, Institute of Cytology and Genetics, Northeast Normal University, Changchun, 130024, China

ABSTRACT

Rnf10 is a member of the RING finger protein family. Recently, a number of RING finger proteins were reported to be involved in neuronal differentiation, development, and proliferation. In this study, we observed that the mRNA levels and protein expression of Rnf10 increase significantly upon the retinoic acid-induced neuronal differentiation of P19 cells. Knockdown of Rnf10 by RNA interference significantly impaired neuronal differentiation of P19 cells by attenuating the expression of neuronal markers. Cell cycle profiling revealed that Rnf10-depleted cells were unable to establish cell cycle arrest after RA treatment. In agreement with flow cytometry analysis, increased cell proliferation was observed after RA induction in Rnf10 knockdown cells as determined by a BrdU incorporation assay. Moreover, like Rnf10, the mRNA levels and protein expression of p21 and p27 also increased upon RA induction. Rnf10 knockdown only resulted in a reduction of p21 expression, while p27 and p57 expression remained unchanged, indicating that Rnf10 may regulate cell cycle exit through the p21 pathway. Ectopic p21 expression partially rescued the effect of Rnf10 depletion on the neuronal differentiation of P19 cells. Collectively, these results showed that increase in Rnf10 expression upon RA induction is necessary for the positive regulation of cyclin kinase inhibitor p21 expression, which leads to cell cycle arrest and is critical for neuronal differentiation. J. Cell. Biochem. 114: 2007–2015, 2013. © 2013 Wiley Periodicals, Inc.

KEY WORDS: RETINOIC ACID; RING FINGER PROTEIN 10; NEURONAL DIFFERENTIATION; P19 EMBRYONIC CARCINOMA CELLS

During neuronal differentiation, stem cells give rise to neural and glial progenitors that in turn differentiate into neurons, astrocytes, and oligodendrocytes. This precise temporal and spatial differentiation of neural subtypes is essential for the final functional assembly of neural circuits [Jessell, 2000; Kintner, 2002]. Cell cycle exit and differentiation are two tightly regulated processes. In response to appropriate signals, cells exit the cell cycle and initiate terminal differentiation. This suggests signaling crosstalk between cyclin-dependent kinases (CDKs), associated cyclins and cyclin-dependent kinase inhibitors (CKI). CDKs are a family of enzymes that are required for cell cycle transitions and regulate the activity of cyclins. The precise regulation of CDKs is essential for controlled cell proliferation and the development of an organism. CKIs are a group of proteins that negatively regulate CDKs and are responsible for cell cycle exit. CKIs comprise two families of inhibitors: the INK4 family and the Cip/Kip family [Besson et al., 2008]. The Cip/Kip family, including p21, p27, and p57, is particularly important in the regulation of neuronal differentiation, neurogenesis, and neuronal migration [Galderisi et al., 2003; Itoh et al., 2007]. An in vitro study provided evidence that p21 overexpression can induce neural differentiation in PC12 cells [Erhardt and Pittman, 1998] and is essential for cell cycle arrest in cortical neurons [Itoh et al., 2007]. In addition, the p21 protein can promote neurite growth [Tanaka et al., 2002] and is also known to be involved in the proper proliferation and differentiation of oligodendrocytes [Zezula et al., 2001]. The key mechanisms controlling the expression and activity of this critical regulator during neuronal differentiation are still being explored.

Conflict of interest: The authors declare no conflict of interest.

Grant sponsor: Program for New Century Excellent Talents in University; Grant number: 111496019; Grant sponsor: National Natural Science Foundation of China; Grant numbers: 31171042, 3127148.

*Correspondence to: Xiaojuan Zhu, Key Laboratory of Molecular Epigenetics of Ministry of Education, Institute of Cytology and Genetics, Northeast Normal University, Changchun 130024, China. E-mail: zhuxj720@nenu.edu.cn

Manuscript Received: 22 December 2012; Manuscript Accepted: 6 March 2013

Accepted manuscript online in Wiley Online Library (wileyonlinelibrary.com): 22 March 2013

DOI 10.1002/jcb.24544 • © 2013 Wiley Periodicals, Inc.

All ring finger proteins contain protein sequence motifs similar to zinc finger domains, which are known to be involved in protein–protein interactions. RING finger proteins play pivotal roles in cell cycle progression, differentiation, development, cell signaling, apoptosis, and oncogenesis. RING finger proteins are essential components of the ubiquitin-proteasome system [Joazeiro and Weissman, 2000] and are implicated in a number of malignancies. Some RING finger proteins are oncogenes, while others are products of tumor suppressor genes. However, a single RING finger protein can also have an opposite role depending upon whether it has multiple targets or if there are multiple roles for specific target proteins [Lipkowitz and Weissman, 2011]. Rnf10 is a member of the RING finger protein family. Previous studies have revealed that it can enhance Meox2 activation of the p21 promoter [Lin et al., 2005]. Moreover, it can also regulate the expression of MAG genes and is required for myelin production in Schwann cells of peripheral nervous system [Hoshikawa et al., 2008]. In the present study, we observed that Rnf10 expression was upregulated during P19 cell neuronal differentiation. Inhibition of Rnf10 expression impaired P19 cell neuronal differentiation and cell cycle exit. We further observed that Rnf10 knockdown resulted in the decreased expression of the cyclin kinase inhibitor p21. Re-expression of p21 partially rescued the effect of Rnf10 knockdown on P19 cell neuronal differentiation. To the best of our knowledge, this is first report that provides direct evidence of Rnf10 function in neuronal differentiation.

MATERIALS AND METHODS

ANIMALS

C57/B6 background mice were sacrificed by cervical dislocation and brain regions (cerebral cortex, hippocampus, thalamus, and corpus striatum) were dissected out by Glowinski and Iversen method [1966].

ANTIBODIES

Anti-MAP2, anti-GFAP antibodies, and anti-β actin were purchased from Sigma–Aldrich. Anti-β III tubulin (TU-20) and anti-BrdU were purchased from Abcam. Anti-Flag (4C5 anti-DDK high affinity antibody) was purchased from Origene. Antibodies for Rnf10, p21, p27, and p57 were purchased from Santa Cruz Biotechnology.

CELL CULTURE AND DIFFERENTIATION

All chemicals for cell culture were purchased from Invitrogen unless otherwise stated. The mouse embryonic carcinoma cell line P19 was cultured and maintained in DMEM/F12 medium supplemented with 10% fetal bovine serum at 37°C. Routine passage was performed every 48 h. Cells were differentiated according to the method of Pachernik et al. [2005]. P19 cells ($5 \times 10^3/cm^2$) were plated on 0.1% gelatin-coated culture dishes, and after 24 h the medium was changed to DMEM/F12 supplemented with ITS reagent and 0.5 μM all-trans retinoic acid (Sigma) without serum. RA treatment was given only for the initial 2 days; cells were then allowed to continue differentiation under serum-free conditions with ITS supplement. Cells were exposed to 10 mM Ara-C (Sigma) before harvesting to inhibit the proliferation of non-neuronal cells.

Primary cultures for mouse cerebellar granule cells were obtained from the cerebellums of 7.5-day old mice. Cells were mechanically dissociated, filtered through a 70 μm nylon mesh filter and then plated on pre-coated poly-L-lysine (100 μg/ml, Sigma) plates. Cells were cultured in Neurobasal medium containing B27 supplement and 2 mM L-glutamine.

REAL-TIME QUANTITATIVE PCR ANALYSIS

Reverse transcription was performed with 5 μg of total RNA using the M-MLV reverse transcriptase kit (Promega). Real-time PCR was carried out with SYBR® Premix Ex Taq™ II (Takara) and the StepOnePlus™ Real-Time PCR System. The following primers were used: **Rnf10**: 5′_CCAGGCTCCCATGCAGACTT_3′ and 5′_GGCGGGAGGAACCAAGCTAT_3′, **P21**: 5′_CGGTGGAACTTTGACTTCGT_3′ and 5′_CAGGGCAGAGGAAGTACTGG_3′, **P27**: 5′_TCAAACGTGAGAGTGTCTAACGG_3′ and 5′_AGGGGCTTATGATTCTGAAAGTCG_3′, **P57**: 5′_CCGCGCAAACGTCTGAGATGAG_3′ and 5′_CACCTTGGGACCAGCGTACTCC_3′, **GAPDH**: 5′_ CAGTGGCAAAGTGGAGATTG_3′ and 5′_AATTTGCCGTGAGTGGAGTC_3′. Relative mRNA expression was calculated with the $2^{-\Delta\Delta Ct}$ method using GAPDH as an endogenous control which was shown in our previous study to be an appropriate normalizing control that does not vary in its level of expression with time and treatments [Sheikh et al., 2013].

WESTERN BLOT ANALYSIS

Brain regions were dissected out as above. Total protein from cells and tissues was isolated using radioimmunopreciptation lysis buffer supplemented with protease inhibitor cocktail (Roche). Protein lysates were centrifuged at 14,000 rpm for 15 min at 4°C. Equal protein quantities for every control and test sample were separated by 12% polyacrylamide gel electrophoresis. Resolved protein bands were electroblotted on polyvinylidene difluoride (PVDF) membrane (Millipore) and then blocked with 5% non-fat dry milk. After sequential incubation with primary and secondary antibodies, blots were visualized using electro-generated chemiluminescence (ECL, Amersham) reagent. Finally, blots were exposed to X-ray film for fluorographic imaging and relative band intensities of proteins were quantified using Image J software (National institute of Health).

CELL TRANSFECTIONS AND TRANSDUCTIONS

Replication-deficient lentiviruses were generated by transient transfection of shRNAs and packaging plasmids (psPAX2 and pMD2G), in 293FT cells using the lipofectamine 2000 reagent (Invitrogen). Short hairpin sequences were cloned into the Hpa1 and Xho1 sites of the pLL3.7 vector. For stable virus infections, pLL3.7 vector was modified by replacing GFP (NheI/EcoRI) with the puromycin resistance gene (HindIII/ClaI) from pBabe-puro vector [Lauring et al., 2008]. The sequence targeting Rnf10 was 5′_GCAAATGTCCCATCTGCTACA_3′, the sequence targeting p21 was 5′_GCAAAGTGTGCCGTTGTCTCT_3′, and the sequence for the negative control was 5′_GTTCCCCCATGCAACAATGTA_3′. Viral supernatant was collected 48–72 h post-transfection and concentrated through ultracentrifugation. P19 cells were infected twice with concentrated viral particles in the presence of 8 μg/ml polybrene. After 48 h, cells were selected and maintained in medium containing (1 μg/ml) puromycin. For p21 overexpression, cells were transfected with Myc-Flag-tagged p21 cDNA and pCMV6 empty vector (Origene) using Fugene6 (Roche) and selected with 300 μg/ml of G418 (Sigma).

IMMUNOFLUORESCENCE STAINING AND CONFOCAL MICROSCOPY

Cells were fixed with 4% paraformaldehyde and then permeabilized with 0.3% Triton X-100. Cells were incubated overnight with primary antibodies at 4°C. Secondary antibody incubation was performed for 1 h at room temperature followed by DAPI counterstaining. Coverslips were mounted and sealed with nail polish. Fluorescence was observed using confocal laser scanning microscopy (Olympus FV 1000).

FLOW CYTOMETRY ANALYSIS OF CELL CYCLE DISTRIBUTION

For cell cycle analysis, 1×10^6 cells were fixed in 75% ethanol for 1 h at room temperature. Cells were then stained with propidium iodide (20 µg/ml) along with (10 mg/ml) RNase treatment for approximately 30 min and analyzed with a flow cytometer.

BrdU INCORPORATION ASSAY

P19 cells, which were differentiated for 4 days, were trypsinized and plated on glass coverslips. BrdU (Sigma–Aldrich) at 40 µM was added to the medium and incubated for 4 h. Cells were then fixed and immunostained with an anti-BrdU antibody.

STATISTICAL ANALYSIS

Each experiment was performed at least three times and data is represented as the mean ± SEM. Statistical analysis was performed using one-way ANOVA to compare the means of groups, and P values <0.05 indicate significant differences.

RESULTS

EXPRESSION OF Rnf10 DURING P19 CELL NEURONAL DIFFERENTIATION, IN CEREBELLAR GRANULAR CELLS AND IN AREAS OF THE MOUSE BRAIN

P19 embryonic carcinoma cells have been widely used to explore the basic aspects of neuronal differentiation. Undifferentiated P19 cells are characterized by high proliferation and gene expression patterns similar to stem cells. Retinoic acid can induce the differentiation of P19 cells into neurons and gliacytes by activating the transcription of many genes encoding transcription factors, cell signaling proteins, structural proteins, enzymes, and cell receptors [Maden, 2001]. Therefore, the expression of neuronal markers, neuronal transmitters and receptors in retinoic acid-induced P19 cells resemble the early in vivo development of neurons [Ulrich and Majumder, 2006]. In this study, Rnf10 expression was examined during P19 neuronal differentiation using real-time quantitative PCR and Western blotting. Rnf10 mRNA expression was significantly increased by retinoic acid differentiation signals compared to undifferentiated cells (Fig. 1A). The results of Rnf10 protein expression were similar to mRNA expression during neuronal differentiation (Fig. 1B,C). These results provided the precise time course of Rnf10 expression and suggested its role during neuronal differentiation. In addition, immunostaining for Rnf10 and MAP2 showed that Rnf10 is predominant in the cell body and nucleus of P19-dreived neurons. To further elucidate the cellular identity of Rnf10 expression, cerebellar granular cells from 7.5-day-old mice were immunostained for Rnf10, MAP2 and GFAP. The results showed high expression of Rnf10 in cerebellar neurons and glial cells. Similar to P19-derived

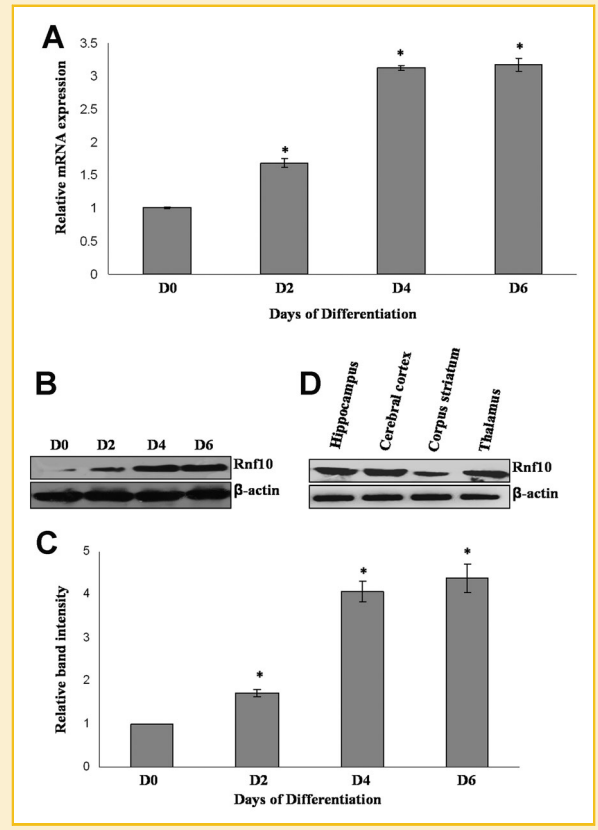

Fig. 1. Expression of Rnf10 during P19 cell neuronal differentiation and in areas of the mouse brain. A: Real-time quantitative PCR analysis of Rnf10. RNA was isolated from undifferentiated P19 cells (D0, RA untreated) and differentiated P19 cells on different days (D2, D4, D6, RA-treated). GAPDH was used as an endogenous control. Error bars represent mean ± SEM. $^*P < 0.05$ versus day 0. For every sample Real-time PCR was performed with four replicates and repeated three times each. B: Western blot analysis for Rnf10 protein expression during RA-induced differentiation of P19 cells. C: Western blots ($n = 3$) were quantified by using Image J software and band intensities were presented relative to Day 0 which is set as 1. Error bars represent mean ± SEM. $^*P < 0.05$ versus Day 0. D: Western blot ($n = 3$) of Rnf10 protein expression in adult (8-week-old) mouse brain regions. β-actin was used as loading control.

neurons, Rnf10 expression in cerebellar neurons was restricted to the cell body and nucleus instead of localizing in specialized structures, that is, axons and dendrites. In contrast, Rnf10 is distributed equally in whole glia indicating its generalized role in glial cells (Fig. 2). Western blot analysis was further performed on tissue from the cerebral cortex, hippocampus, thalamus, and corpus striatum of mice to demonstrate that Rnf10 expression is abundant in brain and may have an important role during neuronal development (Fig. 1D).

Rnf10 KNOCKDOWN RESULTS IN THE IMPAIRED NEURONAL DIFFERENTIATION OF P19-DERIVED NEURONS

Due to the significant increase in Rnf10 expression after retinoic acid-induced neuronal differentiation of P19 cells, we speculated that Rnf10 may have an essential role during neuronal differentiation. To investigate this possibility, we utilized a lentiviral mediated short hairpin Rnf10 knockdown, and a significant reduction in the amount of Rnf10 protein was observed by Western blot compared to negative

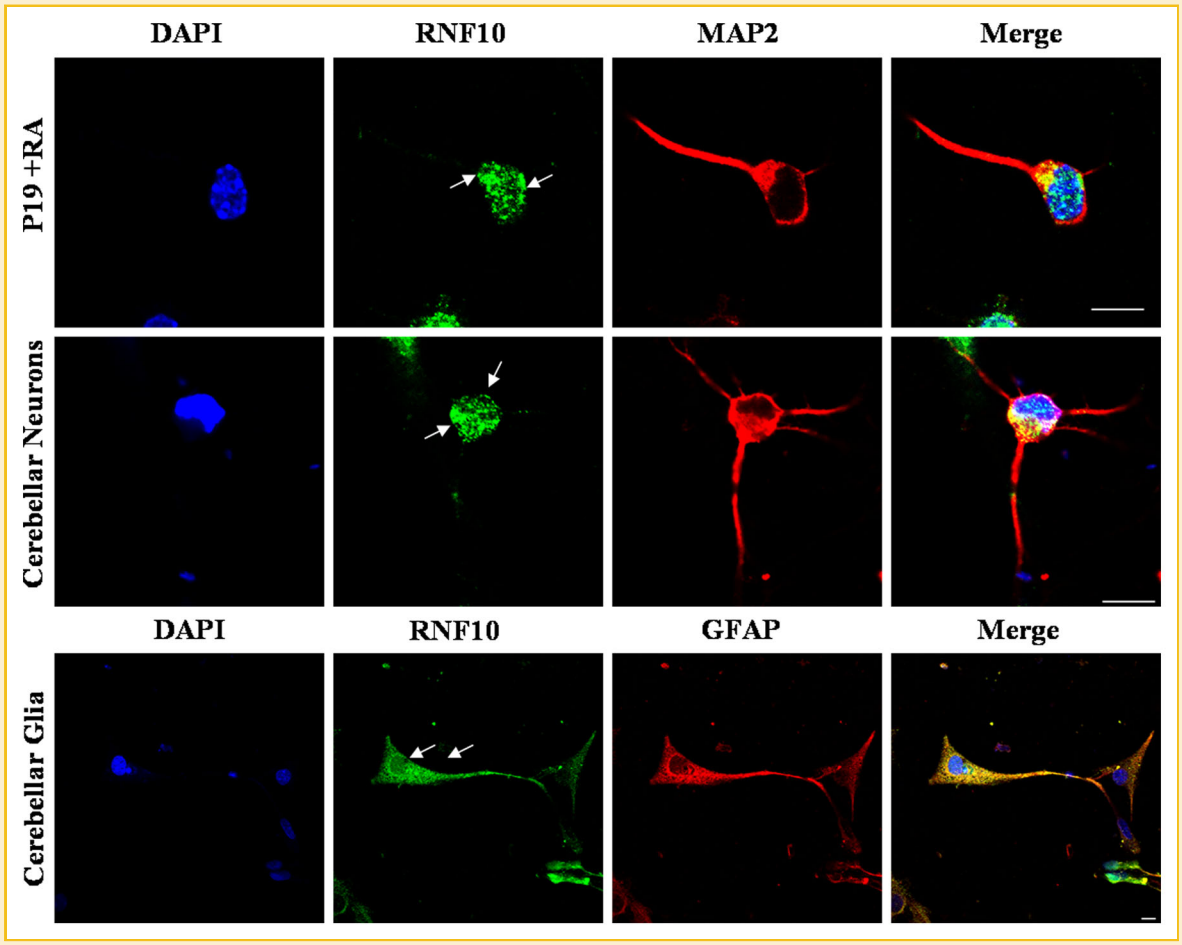

Fig. 2. Subcellular localization of Rnf10 in neuron and glia. Double immunostaining for P19-derived neurons (P19 + RA, 6-day culture), cerebellar granular neurons and glia (6 days in vitro) with Rnf10 and either MAP2 or GFAP antibodies. Cerebellar granular neurons and glia were isolated from 7.5-day-old mouse. Arrow indicates subcellular localization of Rnf10 protein. DAPI is used to stain nuclei. Scale bar 10 μm.

control shRNA (Fig. 3A,B). The effect on neuronal differentiation was observed by the immunofluorescent staining of the neuronal marker MAP2. As shown in Figure 3C, a large number of cells stained for MAP2 in the negative control compared to Rnf10 knockdown cells after differentiation. For quantification analysis, the number of MAP2 positive cells was counted, and the percentage of MAP2 positive cells was calculated. A significant reduction in the percentage of MAP2 positive cells was observed in Rnf10 knockdown cells compared to the negative control (Fig. 3D). A decrease in MAP2 protein expression was also detected by Western blot (Fig. 3A,B). To investigate whether early neuronal differentiation was equally affected in knockdown cells, we detected the early neuronal marker βIII-tubulin by Western blot. Rnf10 shRNA reduced the expression of βIII-tubulin after differentiation, indicating that cell fate was affected even in early stages of neuronal differentiation (Fig. 3A,B).

EFFECT OF Rnf10 DEPLETION ON THE CELL CYCLE PROFILE, CELL PROLIFERATION, AND CYCLIN-DEPENDENT KINASE INHIBITORS

To explore the possibility that Rnf10 may have role in regulating cell cycle exit, which is a prerequisite for terminal differentiation, we investigated the effects of Rnf10 knockdown on cell cycle progression and cell cycle distribution. A BrdU incorporation assay was used to assess cell proliferation by labeling cells in S phase in both Rnf10-depleted cells and control cells. As shown in Figure 3E, cells labeled with BrdU were more numerous with Rnf10 shRNA compared to control shRNA after RA induction. Quantification of BrdU positive cells showed that Rnf10 knockdown cells had a high percentage of BrdU incorporation (S phase) compared to normally differentiating neurons in the negative control (Fig. 3F). Furthermore, we examined cell cycle distribution after Rnf10 depletion using flow cytometry. Normally proliferating P19 embryonic carcinoma cells had an unusually small G0/G1 phase [Fluckiger et al., 2006] as observed in our results. Compared to the RA untreated sh-Neg control, the percentage of G2/M phase cells was increased significantly after RA treatment of the negative control, indicating cell cycle arrest and induction of neuronal differentiation. However, Rnf10 shRNA-infected cells were unable to demonstrate an increase in G2/M RA induction, indicating their inability to establish cell cycle arrest. There was no significant difference in the percentage of G2/M phase cells for RA-treated Rnf10 knockdown cells compared to RA untreated sh-Neg

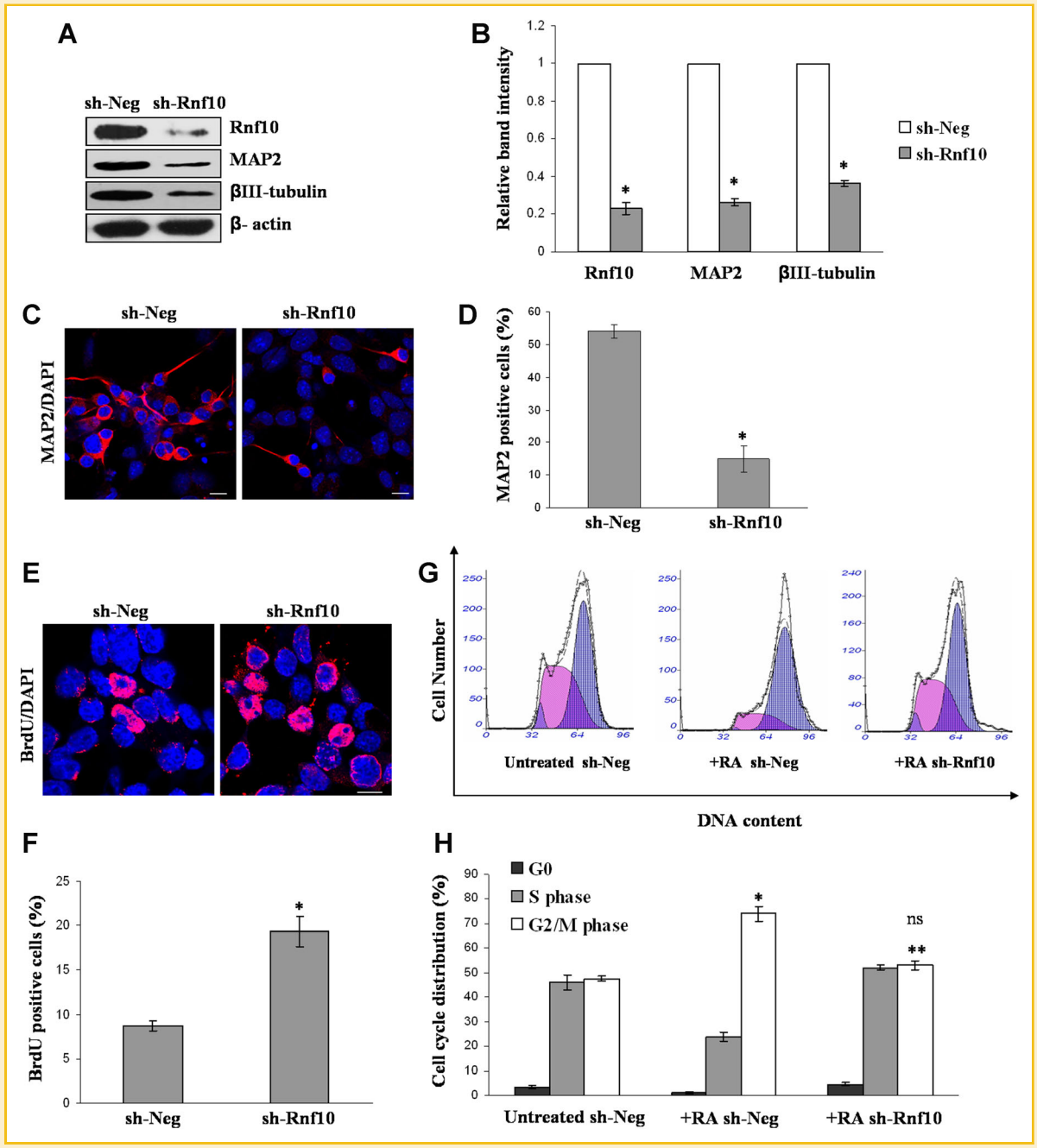

Fig. 3. Rnf10 knockdown inhibits neuronal differentiation and affects the cell cycle profile of P19 cells. A: Western blot analysis of Rnf10, MAP2 and βIII-tubulin proteins in sh-Neg control and sh-Rnf10 virus-infected P19 cells differentiated for 6 days. B: Western blots ($n = 3$) were quantified by using Image J software and band intensities were presented relative to sh-Neg control which is set as 1. Error bars represent mean ± SEM. $^{*}P < 0.05$ versus sh-Neg. β-actin was used as loading control. C: MAP2 immunostaining of P19-derived neurons from sh-Neg and sh-Rnf10 virus-infected P19 cells differentiated for 6 days. D: Percentage of MAP2 positive cells[a]. E: BrdU immunostaining of RA-treated P19 cells infected with sh-Neg control and sh-Rnf10 virus (cultured for 4 days). F: Percentage of BrdU positive cells[b]. DAPI is used to stain nuclei. Scale bar 10 μm. At least 500 cells were counted for each group (sh-Neg and shRnf10). G: Flow cytometry analysis of cell cycle distribution in normally proliferating RA-untreated P19 cells infected with sh-Neg control and RA-treated P19 cells infected with either sh-Neg or sh-Rnf10 lentivirus (cultured for 4 days). Representative of $n = 3$. H: Percentage of cells in each phase of the cell cycle[c]. ns = non-significant difference versus untreated sh-Neg control.[a,b*] $P < 0.05$ versus sh-Neg control. [c*] $P < 0.05$ versus RA-untreated sh-Neg control, $^{**}P < 0.05$ versus RA-treated sh-Neg control. Error bars represent mean ± SEM.

P19 cells, and a high percentage of cells were in the proliferating phase, which correlated well with the BrdU incorporation assay (Fig. 3G,H).

Reduced expression of early and late neuronal markers, increased BrdU incorporation and changes in cell cycle distribution after Rnf10 depletion indicate that proteins involved in cell cycle regulation may have been affected. The Cip/Kip family of proteins, comprising p21, p27, and p57, inhibit a broader spectrum of cyclin-CDK complexes and are particularly important in regulating proliferation and differentiation during neurogenesis. Therefore, to understand the

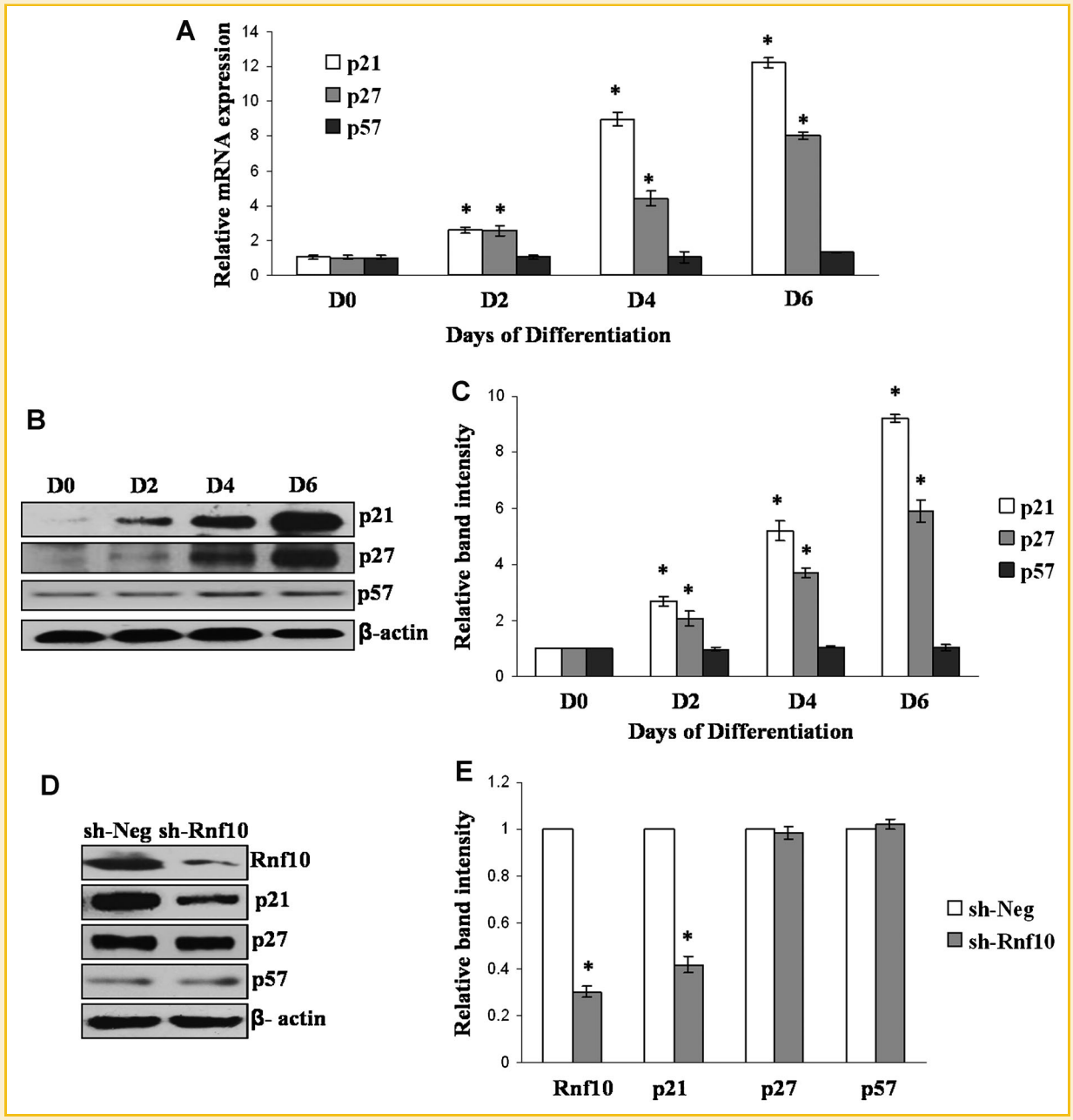

Fig. 4. Expression patterns of Cip/Kip cyclin kinase inhibitors during P19 cell neuronal differentiation and the effects of Rnf10 knockdown on these proteins. A: Real-time quantitative PCR analysis of p21, p27, and p57 during RA-induced differentiation of P19 cells. GAPDH was used as an endogenous control. Error bars represent mean ± SEM. $^{*}P < 0.05$ versus Day 0 (RA untreated). For every sample Real-time PCR was performed with four replicates and repeated three times each. B: Western blot analysis of p21, p27, and p57 during RA-induced differentiation of P19 cells. C: Western blots (n = 3) were quantified by using Image J software and band intensities were presented relative to Day 0 which is set as 1. Error bars represent mean ± SEM. $^{*}P < 0.05$ versus Day 0. D: Western blot analysis of p21, p27, and p57 proteins in sh-Neg control and sh-Rnf10 virus-infected P19 cells differentiated for 6 days. E: Western blots (n = 3) were quantified by using Image J software and band intensities were presented relative to sh-Neg control which is set as 1. Error bars represent mean ± SEM. $^{*}P < 0.05$ versus sh-Neg. β-actin was used as loading control.

effect of Rnf10 knockdown on cell cycle exit and the neuronal differentiation of P19 cells, we selected the Cip/Kip family of cyclin kinase inhibitors for further study. First, we examined the expression of p21, p27, and p57 during RA-induced neuronal differentiation by real-time PCR and Western blot analysis. The results showed that expression of p21 and p27 increased significantly after RA induction, but p57 expression remained the same (Fig. 4A–C). This suggests that p21 and p27 may have more important roles during P19 neuronal differentiation. Furthermore, to investigate the effect of Rnf10 depletion on these CKIs, we detected their protein expression in knockdown cells. The expression of p57 and p27 essentially remained the same; however, the expression of p21 was reduced in Rnf10 knockdown cells (Fig. 4D,E).

THE EFFECT OF p21 KNOCKDOWN WAS SIMILAR TO Rnf10 DEPLETION, AND ITS OVEREXPRESSION CAN PARTIALLY RESCUE NEURONAL DIFFERENTIATION IN Rnf10 KNOCKDOWN CELLS

To investigate whether the reduced expression of p21 after Rnf10 depletion is responsible for increased cell proliferation and impaired neuronal differentiation of RA-induced P19 cells, we knocked down p21 in P19 cells (Fig. 5A). Cells were induced with RA and stained for MAP2, and as we suspected there was decreased MAP2 staining in p21 knockdown cells compared to the scrambled RNA control. Quantitative analysis of MAP2 positive cells also showed a significant reduction in P19-derived neurons from p21 knockdown cells (Fig. 5B,C). Furthermore, there was a significant increase in BrdU incorporation in RA treated p21 knockdown cells compared to the sh-Neg control, indicating that both neuronal differentiation and cell proliferation were affected by p21 knockdown (Fig. 5D,E). These results were similar to the effects of Rnf10 knockdown on neuronal differentiation and proliferation. When Rnf10 knockdown cells were co-transfected with a p21 over-expression vector, a significant increase in MAP2 positive cells was observed compared to Rnf10 knockdown cells transfected with the pCMV6 empty control. Our results also showed that the effect of Rnf10 knockdown on P19 cell neuronal differentiation was partially rescued by p21 ectopic expression when compared with cells transfected with sh-Neg and empty pCMV6 vector (Fig. 5F–H).

DISCUSSION

Cell cycle exit, cell migration, and neuronal differentiation are key steps in the tight regulation of neurogenesis. In this regard, proliferation and differentiation are basic incompatible cellular states, and mitotic cells that do not reprogram after the initiation of neuronal differentiation often undergo cell death. Several in vivo and in vitro studies have been carried out to investigate the transcriptional pathways that control this transition between proliferation and differentiation; however, the regulatory mechanisms for this coherent program of neurogenesis are not yet fully established [Jessell, 2000]. The RING finger proteins, which contain a characteristic C3HC4 or C3H2C3, are in general ubiquitin protein ligases. From the current trajectory of publications, it has become apparent that the ubiquitin-conjugating system has a far greater role in oncogenesis, tumor suppression, cell cycle progression, signal transduction and development than was previously anticipated [Lipkowitz and Weissman, 2011]. These proteins show a variety of biochemical properties, including DNA binding, transactivation, or transrepression; RNA binding; metal-ion binding; or protein binding [Sun et al., 2001]. Recently, ring finger proteins have been reported to play a role in neuronal differentiation and development. For example, BERP is strongly expressed in mouse brain and has been identified as a candidate tumor suppressor gene in humans. Mutation of this RING finger protein was shown to prevent neuronal differentiation and neurite out-growth [Cheung et al., 2010]. In the present study, we identified the role of RING finger protein 10 in the neuronal differentiation of P19 cells. Rnf10 was extensively expressed in mouse brain regions and glial cells as well as neuronal subtypes, which indicates its general role in the central nervous system. Rnf10 contains three putative nuclear localization signals but was previously reported to localize in the cytoplasm of NIH3T3 cells [Seki et al., 2000; Lin et al., 2005]. We report that Rnf10 localizes both in nucleus and cytoplasm of neurons and glia; however, it does not distribute to the specialized structures of neurons. Our study further reveals that Rnf10 acts as a positive regulator of neuronal differentiation, as its knockdown effectively reduced the number of cells expressing early and late neuronal markers. These findings are supported by earlier reports showing that Rnf10 associates with Meox2, which regulates the proliferation, differentiation and migration of vascular smooth muscle cells and cardiomyocytes [Lin et al., 2005]. In agreement with this, Rnf10 is also known to be involved in Schwann cell-specific myelination and differentiation [Hoshikawa et al., 2008].

A number of factors are linked with cell cycle regulation as well as neuronal lineage determination. Recently, the RING finger protein Znf179 was reported to not only be involved in neuronal differentiation but also to modulate cell cycle exit by regulating p27 cyclin kinase inhibitor [Pao et al., 2011]. In this study, we observed that Rnf10 knockdown cells abolished the increase in G2/M phase after RA induction, which implicates its role in cell cycle exit. Along with increases in Rnf10 expression, p21 and p27 expression were also increased upon RA induction. These members of the Cip/Kip family of cyclin-dependent kinase inhibitors (CKIs) are well-characterized for their role in the inhibition of cell cycle progression. In contrast to p27 and p57, p21 has a wide spectrum of inhibitory effects on CDK-cyclin complexes; in particular, it inhibits CDK2 and CDK4, resulting in G1/S cell cycle arrest. It can also inhibit the cyclinA-CDK1/2 and cyclin B1-CDK1 complexes, leading to cell cycle exit at the G2 phase [Jung et al., 2010]. We observed reduced expression of p21 after RA induction of Rnf10 knockdown cells, which indicated that p21 may function downstream of Rnf10 during neuronal differentiation. These findings are supported by previously reported evidence that Rnf10 acts as co-activator for p21 promoter activity in NIH3T3 cells [Lin et al., 2005].

The Cip/Kip family of cyclin kinase inhibitors is known to play their part not only in cell cycle arrest but also in neuronal differentiation. P27 promotes neuronal differentiation and migration [Nguyen et al., 2006], whereas p57 functions in coordination with p27 during cortical development [Itoh et al., 2007]. P21 is already known to promote neural differentiation of PC12 cells and regulate cell cycle exit in cortical neurons [Erhardt and Pittman, 1998; Nguyen et al., 2006]. In addition, p21 is also required for the proliferation and differentiation of oligodendrocytes [Zezula et al., 2001]. We observed that Rnf10 regulates neuronal differentiation through p21, as its expression was reduced in RA-treated Rnf10 knockdown cells, and its ectopic expression partially rescued neuronal differentiation in these cells. This partial rescue of Rnf10 function indicates that other mechanisms may also be involved. Nonetheless, these observations show that Rnf10 can modulate the cell cycle exit and neuronal differentiation of P19 cells through the p21 pathway.

ACKNOWLEDGMENTS

This work was supported by the Program for New Century Excellent Talents in University (111496019), National Natural Science

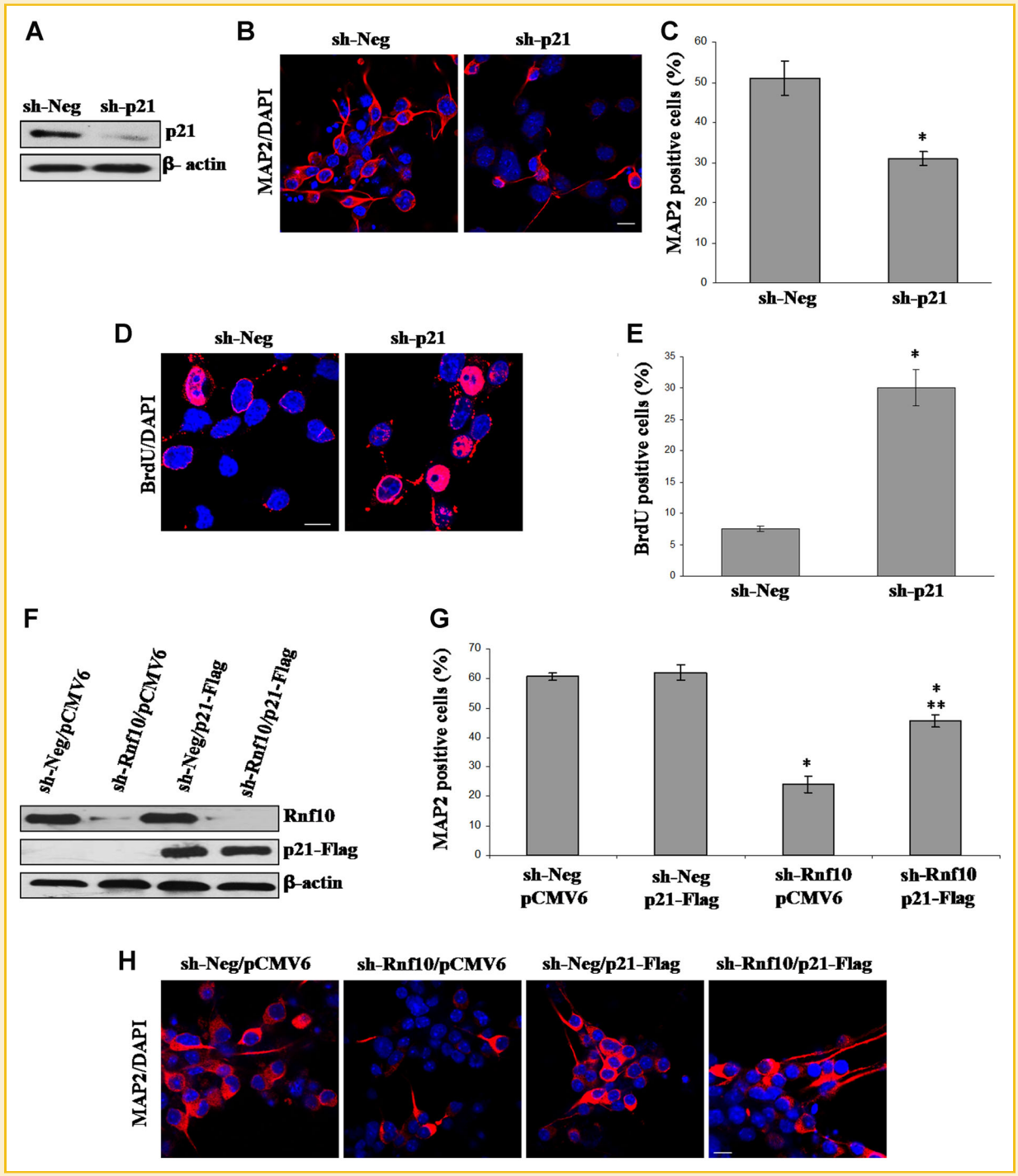

Fig. 5. p21 knockdown increases BrdU incorporation and inhibits neuronal differentiation of P19 cells, and its re-expression partially rescues neuronal differentiation in Rnf10 knockdown cells. A: Western blot analysis ($n = 3$) of p21 protein expression in sh-Neg- and sh-p21-infected P19 cells differentiated for 6 days. B,C: MAP2 immunostaining and the percentage of MAP2 positive cells after p21 knockdown. Cells were cultured for 6 days. $^{*}P < 0.05$ versus sh-Neg control. D,E: BrdU immunostaining and the percentage of BrdU positive cells after p21 knockdown. Cells were cultured for 4 days. At least 500 cells were counted for each group (sh-Neg and shRnf10). $P < 0.05$ versus sh-Neg control. F: Sh-Neg- and shRnf10-infected P19 cells were either transfected with pCMV6 empty vector or p21-Flag-tagged cDNA, and cell extracts were immunoblotted ($n = 3$) using an anti-Rnf10 antibody (top), anti-Flag antibody (middle), and anti-β-actin antibody (bottom). β-actin was used as loading control. G,H: MAP2 percentage and MAP2 immunostaining in cells with the indicated vector expression differentiated for 6 days. At least 500 cells were counted for each group (sh-Neg + pCMV6, sh-Neg + p21-Flag, shRnf10 + pCMV6, and shRnf10 + p21-Flag). $^{*}P < 0.05$ versus sh-Neg + pCMV6 group, $^{**}P < 0.05$ versus sh-Rnf10 + pCMV6 group. DAPI is used to stain nuclei. Scale bar 10 μm. Error bars represent mean ± SEM.

Foundation of China (31171042, 3127148). Sponsors had no role in study design, data collection and analysis, decision to publish, or preparation of the manuscript.

REFERENCES

Besson A, Dowdy SF, Roberts JM. 2008. CDK inhibitors: Cell cycle regulators and beyond. Dev Cell 14:159–169.

Cheung CC, Yang C, Berger T, Zaugg K, Reilly P, Elia AJ, Wakeham A, You-Ten A, Chang N, Li L, Wan Q, Mak TW. 2010. Identification of BERP (brain-expressed RING finger protein) as a p53 target gene that modulates seizure susceptibility through interacting with GABA(A) receptors. Proc Natl Acad Sci USA 107:11883–11888.

Erhardt JA, Pittman RN. 1998. Ectopic p21(WAF1) expression induces differentiation-specific cell cycle changes in PC12 cells characteristic of nerve growth factor treatment. J Biol Chem 273:23517–23523.

Fluckiger AC, Marcy G, Marchand M, Negre D, Cosset FL, Mitalipov S, Wolf D, Savatier P, Dehay C. 2006. Cell cycle features of primate embryonic stem cells. Stem Cells 24:547–556.

Galderisi U, Jori FP, Giordano A. 2003. Cell cycle regulation and neural differentiation. Oncogene 22:5208–5219.

Glowinski J, Iversen LL. 1966. Regional studies of catecholamines in the rat brain. I. The disposition of [3H]norepinephrine, [3H]dopamine and [3H]dopa in various regions of the brain. J Neurochem 13:655–669.

Hoshikawa S, Ogata T, Fujiwara S, Nakamura K, Tanaka S. 2008. A novel function of RING finger protein 10 in transcriptional regulation of the myelin-associated glycoprotein gene and myelin formation in Schwann cells. PLoS ONE 3:e3464.

Itoh Y, Masuyama N, Nakayama K, Nakayama KI, Gotoh Y. 2007. The cyclin-dependent kinase inhibitors p57 and p27 regulate neuronal migration in the developing mouse neocortex. J Biol Chem 282:390–396.

Jessell TM. 2000. Neuronal specification in the spinal cord: Inductive signals and transcriptional codes. Nat Rev Genet 1:20–29.

Joazeiro CA, Weissman AM. 2000. RING finger proteins: Mediators of ubiquitin ligase activity. Cell 102:549–552.

Jung YS, Qian Y, Chen X. 2010. Examination of the expanding pathways for the regulation of p21 expression and activity. Cell Signal 22:1003–1012.

Kintner C. 2002. Neurogenesis in embryos and in adult neural stem cells. J Neurosci 22:639–643.

Lauring J, Abukhdeir AM, Konishi H, Garay JP, Gustin JP, Wang Q, Arceci RJ, Matsui W, Park BH. 2008. The multiple myeloma associated MMSET gene contributes to cellular adhesion, clonogenic growth, and tumorigenicity. Blood 111:856–864.

Lin J, Friesen MT, Bocangel P, Cheung D, Rawszer K, Wigle JT. 2005. Characterization of Mesenchyme Homeobox 2 (MEOX2) transcription factor binding to RING finger protein 10. Mol Cell Biochem 275:75–84.

Lipkowitz S, Weissman AM. 2011. RINGs of good and evil: RING finger ubiquitin ligases at the crossroads of tumour suppression and oncogenesis. Nat Rev Cancer 11:629–643.

Maden M. 2001. Role and distribution of retinoic acid during CNS development. Int Rev Cytol 209:1–77.

Nguyen L, Besson A, Heng JI, Schuurmans C, Teboul L, Parras C, Philpott A, Roberts JM, Guillemot F. 2006. p27kip1 independently promotes neuronal differentiation and migration in the cerebral cortex. Genes Dev 20:1511–1524.

Pachernik J, Bryja V, Esner M, Kubala L, Dvorak P, Hampl A. 2005. Neural differentiation of pluripotent mouse embryonal carcinoma cells by retinoic acid: Inhibitory effect of serum. Physiol Res 54:115–122.

Pao PC, Huang NK, Liu YW, Yeh SH, Lin ST, Hsieh CP, Huang AM, Huang HS, Tseng JT, Chang WC, Lee YC. 2011. A novel RING finger protein, Znf179, modulates cell cycle exit and neuronal differentiation of P19 embryonal carcinoma cells. Cell Death Differ 18:1791–1804.

Seki N, Hattori A, Sugano S, Muramatsu M, Saito T. 2000. cDNA cloning, expression profile, and genomic structure of human and mouse RNF10/Rnf 10 genes, encoding a novel RING finger protein. J Hum Genet 45:38–42.

Sheikh MA, Malik YS, Yu H, Lai M, Wang X, Zhu XJ. 2013. Epigenetic regulation of Dpp6 Expression by Dnmt3b and its novel role in the inhibition of RA induced neuronal differentiation of P19 cells. PLoS ONE 8: e55826.

Sun Y, Tan M, Duan H, Swaroop M. 2001. SAG/ROC/Rbx/Hrt, a zinc RING finger gene family: Molecular cloning, biochemical properties, and biological functions. Antioxid Redox Signal 3:635–650.

Tanaka H, Yamashita T, Asada M, Mizutani S, Yoshikawa H, Tohyama M. 2002. Cytoplasmic p21(Cip1/WAF1) regulates neurite remodeling by inhibiting Rho-kinase activity. J Cell Biol 158:321–329.

Ulrich H, Majumder P. 2006. Neurotransmitter receptor expression and activity during neuronal differentiation of embryonal carcinoma and stem cells: From basic research towards clinical applications. Cell Prolif 39: 281–300.

Zezula J, Casaccia-Bonnefil P, Ezhevsky SA, Osterhout DJ, Levine JM, Dowdy SF, Chao MV, Koff A. 2001. p21cip1 is required for the differentiation of oligodendrocytes independently of cell cycle withdrawal. EMBO Rep 2: 27–34.